JOURNAL OF VIROLOGY, Jan. 2006, p. 891–899 Vol. 80, No. 2
0022-538X/06/$08.00+0 doi:10.1128/JVI.80.2.891–899.2006

Potent Neutralization of Hendra and Nipah Viruses by Human Monoclonal Antibodies

Zhongyu Zhu,[1,2] Antony S. Dimitrov,[3] Katharine N. Bossart,[3]† Gary Crameri,[4] Kimberly A. Bishop,[3] Vidita Choudhry,[1] Bruce A. Mungall,[4] Yan-Ru Feng,[3] Anil Choudhary,[3] Mei-Yun Zhang,[1,2] Yang Feng,[1] Lin-Fa Wang,[4] Xiaodong Xiao,[1] Bryan T. Eaton,[4] Christopher C. Broder,[3]* and Dimiter S. Dimitrov[1]*

Protein Interactions Group, CCRNP, CCR, NCI-Frederick, NIH, Frederick, Maryland 21702[1]; BRP, SAIC-Frederick, Inc., NCI-Frederick, Frederick, Maryland 21702[2]; Department of Microbiology and Immunology, Uniformed Services University, Bethesda, Maryland 20814[3]; and CSIRO Livestock Industries, Australian Animal Health Laboratory, Geelong, Victoria 3220, Australia[4]

Received 28 August 2005/Accepted 19 October 2005

***Hendra virus* (HeV) and *Nipah virus* (NiV) are closely related emerging viruses comprising the *Henipavirus* genus of the *Paramyxovirinae*. Each has a broad species tropism and can cause disease with high mortality in both animal and human hosts. These viruses infect cells by a pH-independent membrane fusion event mediated by their attachment (G) and fusion (F) envelope glycoproteins (Envs). Seven Fabs, m101 to -7, were selected for their significant binding to a soluble form of Hendra G (sG) which was used as the antigen for panning of a large naïve human antibody library. The selected Fabs inhibited, to various degrees, cell fusion mediated by the HeV or NiV Envs and virus infection. The conversion of the most potent neutralizer of infectious HeV, Fab m101, to immunoglobulin G1 (IgG1) significantly increased its cell fusion inhibitory activity: the 50% inhibitory concentration was decreased more than 10-fold to approximately 1 μg/ml. The IgG1 m101 was also exceptionally potent in neutralizing infectious HeV; complete (100%) neutralization was achieved with 12.5 μg/ml, and 98% neutralization required only 1.6 μg/ml. The inhibition of fusion and infection correlated with binding of the Fabs to full-length G as measured by immunoprecipitation and less with binding to sG as measured by enzyme-linked immunosorbent assay and Biacore. m101 and m102 competed with the ephrin-B2, which we recently identified as a functional receptor for both HeV and NiV, indicating a possible mechanism of neutralization by these antibodies. The m101, m102, and m103 antibodies competed with each other, suggesting that they bind to overlapping epitopes which are distinct from the epitopes of m106 and m107. In an initial attempt to localize the epitopes of m101 and m102, we measured their binding to a panel of 11 G alanine-scanning mutants and identified two mutants, P185A and Q191 K192A, which significantly decreased binding to m101 and one, G183, which decreased binding of m102 to G. These results suggest that m101 to -7 are specific for HeV or NiV or both and exhibit various neutralizing activities; they are the first human monoclonal antibodies identified against these viruses and could be used for treatment, prophylaxis, and diagnosis and as research reagents and could aid in the development of vaccines.**

Nipah virus (NiV) and *Hendra virus* (HeV) are closely related emerging paramyxoviruses that comprise the *Henipavirus* genus (1, 12–15, 18, 21, 27, 28, 30). Paramyxoviruses are negative-sense RNA-containing enveloped viruses and contain two major membrane-anchored envelope glycoproteins that are required for infection of a receptive host cell. All members contain an F glycoprotein which mediates pH-independent membrane fusion between the virus and its host cell, while the second attachment glycoprotein can be either a hemagglutinin-neuraminidase protein (HN), a hemagglutinin protein (H), or a G glycoprotein, depending on the particular virus (reviewed in reference 26). As with all paramyxoviruses, the fusion and attachment glycoproteins are also the principal antigens to which virtually all neutralizing antibodies are directed.

The broad species tropisms and the ability to cause fatal disease in both animals and humans distinguish HeV and NiV from all other known paramyxoviruses (reviewed in reference 17). They are biological safety level 4 (BSL-4) pathogens and are on the National Institute of Allergy and Infectious Diseases biodefense research agenda as zoonotic emerging category C priority pathogens that could be used as bioterror agents. The henipaviruses can be amplified and cause disease in large animals and be transmitted to humans, where disease can be a severe respiratory illness and febrile encephalitis. They can be readily grown in cell culture or embryonated chicken eggs, produce high unconcentrated titers ($\sim 10^8$) 50% tissue culture infective doses ($TCID_{50}$)/ml (16), and are highly infectious (20, 23).

NiV has reemerged on several occasions in Bangladesh. Two recent outbreaks of NiV in 2004 have been confirmed, and yet another one occurred in January of 2005 (4). Several important observations in these most recent outbreaks have been made, including a higher incidence of acute respiratory distress syn-

* Corresponding author. Mailing address for D. S. Dimitrov: CCRNP, CCR, NCI-Frederick, NIH, Bldg. 469, Rm. 105, Frederick, MD 21702-1201. Phone: (301) 846-1352. Fax: (301) 846-5598. E-mail: dimitrov@ncifcrf.gov. Mailing address for C. C. Broder: Department of Microbiology and Immunology, Uniformed Services University, Bethesda, MD 20814. Phone: (301) 295-3401. Fax: (301) 295-1545. E-mail: cbroder@usuhs.mil.

† Present address: CSIRO Livestock Industries, Australian Animal Health Laboratory, Geelong, Victoria 3220, Australia.

drome, person-to-person transmission, and significantly higher case fatality rates (60 to 75%), in contrast to the Malaysian outbreak (about 40%), where the virus was discovered or suspected to have originated (2, 3, 11, 19, 24). There are currently no therapeutic modalities for treating NiV or HeV infections, and a vaccine for prevention of disease in human or livestock populations does not exist. Although antibody responses were detected in infections caused by these viruses, human monoclonal antibodies (hMAbs) have not been identified against either virus. A number of studies have shown the importance of neutralizing antibodies in recovery and protection from viral infections (17). Therefore, the development of neutralizing hMAbs against NiV and HeV could have important implications for prophylaxis and passive immunotherapy. In addition, the characterization of the epitopes of the neutralizing antibodies could provide helpful information for development of candidate vaccines and drugs. Finally, such antibodies could be used for diagnosis and as research reagents.

Here, we report the identification of potent neutralizing hMAbs targeting the viral envelope glycoprotein G by using a highly purified, oligomeric, soluble HeV G (sG) glycoprotein as the antigen for screening of a large naïve human phage display library. One of these antibodies exhibited exceptional potency against infectious HeV, and another one neutralized both HeV and NiV. Because these antibodies are fully human antibodies, they could be directly used for prophylaxis and treatment of humans infected with HeV or NiV.

MATERIALS AND METHODS

Cells and culture conditions. HeLa-USU cells were provided by Anthony Maurelli, Uniformed Services University (USU). HeLa-ATCC cells were obtained from the American Type Culture Collection (ATCC CCL 2). Vero cells were provided by Alison O'Brien, USU. The human glioblastoma cell line U373-MG was provided by Adam P. Geballe, Fred Hutchinson Cancer Research Center. The human head and neck carcinoma PCI 13 cell line was a gift of Ernest Smith, Vaccinex, Inc. HeLa-USU, HeLa-ATCC, and U373 cells were maintained in Dulbecco's modified Eagle's medium (Quality Biologicals, Gaithersburg, Md.) supplemented with 10% cosmic calf serum (CCS; HyClone, Logan, UT) and 2 mM L-glutamine (DMEM-10). PCI 13 cells were maintained in DMEM-10 supplemented with 1 mM HEPES (Quality Biologicals). Vero cells were maintained in Eagle's minimal essential medium (EMEM; Quality Biologicals) supplemented with 10% CCS (HyClone) and 2 mM L-glutamine (EMEM-10). All cell cultures were maintained at 37°C in a humidified 5% CO_2 atmosphere.

Alanine G mutants. Alanine mutations were made at specific residues in myc-tagged HeV G using site-directed mutagenesis (Stratagene). All mutants were sequenced and tested for expression. Plasmids containing either mutant or wild-type HeV myc-tagged G were transfected into HeLa-USU monolayers using Fugene (Roche) and incubated overnight. The immunoprecipitation of the mutant G was performed as described below in "Immunoprecipitation," except that 3.0 μg of either m101 or m102 or 5 μl of rabbit polyclonal anti-sHeV (α-sHeV) G serum was incubated with 80 μl lysates overnight at 4°C, followed by precipitation at room temperature with 100 μl 20% protein G-Sepharose for 45 min.

Selection of G-specific phage-displayed Fabs. A naïve human Fab phage display library (a total of about 10^{10} members), constructed from peripheral blood B cells of 10 healthy donors (Z. Y. Zhu and D. S. Dimitrov, unpublished data), was used for selection of Fabs against purified, soluble, and oligomeric HeV G glycoprotein (7) conjugated to magnetic beads (Dynabeads M-270 epoxy; DYNAL Inc., New Hyde Park, N.Y.). Amplified libraries of 10^{12} phage-displayed Fabs were incubated with 5, 3, 3, and 1 μg of sG in a 500-μl volume for 2 h at room temperature during the first, second, third, and fourth rounds of biopanning, respectively. After each round of incubation the beads were washed 5 times for the first round and 15 times for the later rounds with phosphate-buffered saline containing 0.05% Tween 20 (PBST) to remove nonspecifically bound phage, the bead-bound phage were mixed with TG1 cells for 1 hour at 37°C, and the phage was amplified from the infected cells and used in the next round of biopanning. After the fourth round of biopanning, 380 clones were randomly picked from the infected TG1 cells and each inoculated into 150 μl 2YT medium containing 100 μg/ml carbenicillin and 0.2% glucose in 96-well plates by using the automated BioRobotics BioPick colony picking system (Genomic Solutions, Ann Arbor, MI). After the bacterial cultures reached an optical density at 600 nm (OD_{600}) of 0.5, helper phage M13K07 at a multiplicity of infection (MOI) of 10 and kanamycin at 50 μg/ml (final concentration) were added to the medium, and the plates were further incubated at 30°C overnight in a shaker at 250 rpm. The phage supernatants were mixed with 3% nonfat milk in PBS at a 4:1 volume ratio and used for enzyme-linked immunosorbent assay (ELISA) to identify clones of phage displaying Fabs with high sG binding affinity. The supernatants were incubated for 2 h at room temperature with sG protein coated at 50 ng per well in 96-well plates and washed five times with PBST. (sG was coated in 50 μl coating buffer [50 mM NaHCO3, pH 9.6]; after overnight incubation at 4°C it was blocked with 3% nonfat milk in PBS and washed three times with PBS containing 0.05% Tween 20.) sG-bound phage were detected by using horseradish peroxidase-conjugated goat anti-M13 antibody. After incubation with the antibody, the nonspecifically bound antibody was washed, the 3,3′5,5′-tetramethylbenzidine (TMB) substrate was added, and the solution absorbance at 450 nm (A_{450}) was measured. Clones that bound to sG with A_{450} of >1.0 were selected for further characterization.

Expression and purification of selected soluble Fabs. The VH and VL of the selected clones were sequenced, and the Fabs encoded by clones with unique sequences were expressed and purified as described below. Plasmids extracted from these clones were used for transformation of HB2151 cells. A single colony was picked from the plate containing freshly transformed cells, inoculated into 200 ml 2YT medium containing 100 μg/ml ampicillin and 0.2% glucose, and incubated at 37°C with shaking at 250 rpm. When the culture OD at 600 nm reached 0.90, isopropyl-β-D-thiogalactopyranoside at a 0.5 mM final concentration was added, and the culture was further incubated overnight at 30°C. The bacterial pellet was collected after centrifugation at 8,000 × *g* for 20 min and resuspended in PBS buffer containing 0.5 mU polymixin B (Sigma-Aldrich, St. Louis, MO). After 30 min incubation with rotation at 50 rpm at room temperature, it was centrifuged at 25,000 × *g* for 25 min at 4°C, and the supernatant was used for Fab purification with a protein G column (Sigma-Aldrich, St. Louis, MO).

Conversion of Fab to IgG1 and IgG1 expression and purification. The Fab heavy and light chains were amplified and recloned in the PDR12 vector (provided by D. Burton, Scripps Research Institute, La Jolla, CA) for whole immunoglobulin G1 (IgG1) expression. The resulting construct was transfected, and the IgG1 was expressed using the FreeStyle 293 expression kit following the protocol from the manufacturer (Invitrogen, Carlsbad, CA). The IgG1 was purified from the culture medium with a protein G column (Sigma-Aldrich, St. Louis, MO).

Affinity determination by surface plasmon resonance. Interactions between various Fabs and G were analyzed by surface plasmon resonance technology using a BIACORE 1000 instrument (Biacore; Pharmacia, Piscataway, NJ). sG was covalently immobilized onto a sensor chip (CM5) using carbodiimide coupling chemistry. A control reference surface was prepared for nonspecific binding and refractive index changes. For analysis of the kinetics of interactions, various concentrations of Fabs (300, 100, 33, 11, and 3.7 nM) were injected at a flow rate of 30 μl/min using running buffer containing 150 mM NaCl, 3 mM EDTA, and 0.005% P-20 (pH 7.4). The association and dissociation phase data were fitted simultaneously to a 1:1 Langumir global model by using the nonlinear data analysis program BIAevaluation 3.2. All the experiments were performed at 25°C.

Competition ELISA. The Fabs m101, m102, m103, m106, and m107 were coated at 150, 50, 300, 300, and 100 ng per well, respectively, in 50 μl coating buffer as described above for sG, blocked with nonfat milk, and washed. c-Myc-tagged sG mixed with each of the Fabs in blocking buffer at final concentrations of 5 μg/ml and 20 μg/ml, respectively, was added to each of the Fab-coated wells; sG (5 μg/ml) without antibody was added to each of the coated Fabs as a positive control. Bound c-Myc-tagged sG protein was detected by a horseradish peroxidase-conjugated anti-c-Myc antibody (Roche Diagnostics Corporation, Indianapolis, IN), the TMB substrate (Sigma-Aldrich, St. Louis, MO) was added, and A_{450} was measured.

Competition between antibodies and the receptor for HeV and NiV, ephrin-B2, for binding to HeV G was measured by using a recombinant mouse ephrin-B2/FC chimera (R&D Systems, Minneapolis, Minn.) coated in a coating buffer at 50 ng per well at 4°C overnight, blocked with 3% nonfat milk in PBS, and washed with PBST. c-Myc-tagged Hendra G protein at final concentration of 1 μg/ml was incubated with serially diluted anti-HeV G antibodies and a control Fab antibody specific for the severe acute respiratory syndrome coronavirus S protein, and the mixtures were added to ephrin-B2-coated wells in duplicates. After washing, bound c-Myc-tagged G protein was detected as described above.

Immunoprecipitation. HeLa-USU monolayers were infected with wild-type vaccinia virus (WR) or recombinant vaccinia virus expressing myc-tagged HeV G

or NiV G at an MOI of 10 for 6 h and then washed twice and incubated overnight in methionine- and cysteine-free essential medium plus 2.5% dialyzed fetal calf serum (Invitrogen) and 100 μCi of [^{35}S]ProMix/ml (Amersham Pharmacia Biotech, Piscataway, NJ). Cells were lysed in 100 mM Tris-HCl (pH 8.0), 100 mM NaCl, and 1% Triton X-100. Lysates were incubated with each Fab at a concentration of 1 μg per 100 μl of lysate for at least 1 hour at 4°C, followed by precipitation at room temperature with 100 μl 20% protein G-Sepharose (Amersham) for 45 min. Anti-Myc antibody 9E10 (Roche Molecular Biochemicals) was used at a concentration of 2 μg per 100 μl of lysate. Samples were washed twice with lysis buffer followed by one wash with deoxycholate buffer containing 100 mM Tris-HCl (pH 8.0), 100 mM NaCl, 0.1% sodium deoxycholate, and 0.1% sodium dodecyl sulfate (SDS). Samples were boiled in SDS-polyacrylamide gel electrophoresis (SDS-PAGE) sample buffer with 2-mercaptoethanol and analyzed by SDS-PAGE and autoradiography.

Cell fusion assays. Fusion between HeV and NiV F and G envelope glycoprotein-expressing cells (effector cells) and target cells was measured by two assays: first, a reporter gene assay in which the cytoplasm of one cell population contained vaccinia virus-encoded T7 RNA polymerase and the cytoplasm of the other contained the *Escherichia coli lacZ* gene linked to the T7 promoter (β-galactosidase [β-Gal] is synthesized only in fused cells [6, 32]); second, a syncytium assay. Typically, the expression of HeV and NiV F and G is performed in a HeV and NiV fusion and an infection-negative HeLa cell line derivative (HeLa-USU). Cytogenetic analysis has confirmed that the HeLa-USU cell line resistant to NiV and HeV mediates membrane fusion, and live virus infection is derived from the ATCC (CCL-2) HeLa cell line (data not shown). Vaccinia virus-encoded proteins (9) were produced by infecting cells at an MOI of 10 and incubating infected cells at 31°C overnight. Cell fusion reactions were conducted with the various cell mixtures in 96-well plates at 37°C. Typically, the ratio of envelope glycoprotein-expressing cells to target cells was 1:1 (2×10^5 total cells per well; 0.2-ml total volume). Cytosine arabinoside (40 μg/ml) was added to the fusion reaction mixture to reduce nonspecific β-Gal production. For quantitative analyses, Nonidet P-40 was added (0.5% final) at 2.5 h, and aliquots of the lysates were assayed for β-Gal at ambient temperature with the substrate chlorophenol red–D-galactopyranoside (Roche Diagnostics Corp., Indianapolis, IN). For inhibition by antibodies, serial antibody dilutions were made and added to effector cell populations 30 min prior to the addition of target cell populations. All assays were performed in duplicate, and fusion data were calculated and expressed as rates of β-Gal activity (change in OD at 570 nm per minute × 1,000) (32). They were normalized with respect to cell fusion in the absence of antibodies and plotted as function of the antibody concentration.

The syncytium assay was performed in 48-well plates. Target PCI-13 cells were plated to reach 80% confluence at the time of the experiment. Effector cells, HeLa-USU, which are nonpermissive to HeV Env- and NiV Env-mediated fusion, were infected with recombinant vaccinia virus to express HeV G and F proteins. Three wells of a six-well plate with 80% confluent HeLa-USU were incubated with both recombinant vaccinia viruses, encoding HeV G and HeV F, at an MOI of 10 for each virus at 37°C for 3 h in DMEM-10 containing 2.5% cosmic calf serum, 1 ml per well, then washed once and dissociated from the plates by using 0.5 ml per well enzyme-free PBS-based cell dissociation buffer (Invitrogen Corp., Carlsbad, CA). The cells were gathered into 50-ml sterile centrifuge tubes (Corning Inc., Corning, NY), and 20 ml DMEM-10 was added. The suspension was incubated 16 h at 31°C in a humidified 5% CO_2 atmosphere. Before the experiment, the cells were centrifuged at 1,200 rpm for 5 min, and the pellet was resuspended in DMEM-10. The cells were counted, centrifuged again, and resuspended at a concentration of 2×10^6 cells/ml. Cytosine arabinoside was added to a concentration of 80 μg/ml. A 100-μl aliquot of this cell suspension was mixed with the same amount of DMEM-10 containing the antibody and incubated for 20 min at room temperature. The mixtures were added to the freshly washed (with DMEM-10) PCI-13 target cells in the 48-well plate and incubated for 3 h at 37°C in a humidified 5% CO_2 atmosphere. Photographs were taken by using the phase-contrast mode of an Olympus IX81 microscope with a 10× objective lens and then electronically amplified whenever needed.

HeV and NiV neutralization assays. All live virus experiments were conducted under strict biocontainment procedures in a BSL-4 laboratory. The full-length IgG1 m101 antibody was evaluated for neutralization of infectious virus by using an immunostaining plaque assay as previously described (8). A total of 2×10^4 Vero cells were added to wells in 150 μl EMEM-10 in a 96-well plate and incubated at 37°C overnight in a humidified 5% CO_2 atmosphere. Antibodies were diluted in EMEM-10 by doubling dilution, and an equal volume of HeV was added to each dilution and incubated at 37°C for 30 min. The titer of HeV was 1.0×10^8 $TCID_{50}$/ml. Virus dilutions were done in EMEM-10 and chosen to generate approximately 50 plaques following adsorption of virus for 30 min at 37°C to Vero cell monolayers (1.5×10^3 $TCID_{50}$/ml for HeV). Antibody-virus mixtures were added to Vero cell monolayers in quadruplicate and incubated for 30 min at 37°C in a humidified 5% CO_2 atmosphere. After 30 min of incubation, antibody-virus mixtures were removed and cells were washed three times with Ca^{2+}-Mg^{2+}-free PBS. Two different variations of this assay were conducted. In the first, EMEM-10 was added to Vero cells after washing and incubated for 18 h. In the second, the same antibody dilution as both the preincubation and virus incubation were added to the respective wells and incubated 18 h. For both assays, the culture medium was discarded the next day, and plates were immersed in ice-cold absolute methanol for 20 min prior to air drying outside the BSL-4 facility. Fixed chamber slides were either stored overnight at 4°C or immunolabeled immediately with anti-phosphoprotein (P) monospecific antiserum. Wells were washed in 0.01 M PBS, pH 7.2, containing 1% bovine serum albumin (BSA) for 5 min. Forty microliters of anti-P antiserum (1:200 in PBS-BSA) was applied to each well and incubated at 37°C for 30 min. Slides were rinsed with PBST and washed for 5 min in PBS-BSA. Forty microliters of fluorescein isothiocyanate-labeled goat anti-rabbit antiserum (ICN Pharmaceuticals, Costa Mesa, Calif.) diluted 1:200 in PBS-BSA containing 4′,6′-diamidino-2-phenylindole (10 μg/ml) was then applied to each well and incubated at 37°C for 30 min. Wells were rinsed again with PBST and washed for 5 min in PBS-BSA. Wells were overlaid with 100 μl glycerol-PBS (9:1) containing DABCO (25 μg/ml) and stored in the dark prior to imaging. Fluorescein isothiocyanate immunofluorescence was visualized using an Olympus IX71 inverted microscope (Olympus Australia, Mt. Waverley, Australia). Percent neutralization at a given antibody concentration was calculated based on the ratio of the average number of fluorescent foci per well in the presence of antibody to the average number observed in the positive control (no antibody) multiplied by 100.

Neutralization of HeV and NiV by Fabs was performed as follows. Fabs were diluted in EMEM-10 by doubling dilution, and an equal volume of EMEM-10 containing 200 $TCID_{50}$ of either HeV or NiV was added to each dilution and incubated at 37°C for 30 min. The titer of HeV was 1.0×10^8 $TCID_{50}$/ml, and the NiV titer was 3.0×10^7 $TCID_{50}$/ml. A total of 2×10^4 Vero cells were added to each Fab-virus mixture in six replicate wells and incubated for 5 days. The percent neutralization of each Fab was determined based on the level of cytopathic effect (CPE) (foci) in replicate wells at each Fab concentration and calculated based on the reduction in the average number of foci per well to the average number of foci observed in the positive control (no Fab) multiplied by 100.

RESULTS

Selection of phage-displayed Fabs (m101 to -7) specific for Hendra virus sG. Our initial efforts to develop G-specific hMAbs by using cell-associated G and synthetic antibody libraries as well as an immune library constructed from frozen lymphocytes of a survivor from Nipah virus infection have not been successful. To develop hMAbs against the G envelope glycoprotein of HeV and NiV, we used a large naïve human Fab library containing about 10^{10} different phage-displayed Fabs we have recently developed (Zhu and Dimitrov, unpublished). Here, we have made use of a unique soluble and secreted form of the attachment (G) glycoprotein of HeV (sG) which we have recently produced and characterized (7). This protein was used as an antigen for screening of the antibody library. After four rounds of panning, screening of 380 individual phage clones was performed in a phage ELISA with sG as described in Materials and Methods. Of those 71 clones that exhibited significant binding to sG and were sequenced, 17 Fabs had unique sequences (Table 1); they were expressed in bacteria, purified, and tested for binding activity. Seven Fabs, designated m101 through m107, exhibited significant ($A_{450} > 0.5$) binding to sG in the ELISA (Table 1). Notably, the heavy chain CDR3s (H3) of the strongest binders (m101, m102, and m106) were significantly longer than the other Fabs that bound more weakly (Table 1). Interestingly, the heavy chains of m101 and m102 (the most potent HeV and NiV neutralizers [see below]) were the most divergent from the germ line heavy chains, indicating a certain level of maturation, although they

TABLE 1. Selection of phage clones with unique sequences that exhibit significant binding to sG[a]

Fab	H3 sequence	A_{450}
m101	D P G G Y S Y G P Y Y Y Y Y G M D V	1.0
m102	G W G R E Q L A P H P S Q Y Y Y Y Y Y G M D V	1.4
m103	D S R Y H D A F D I	0.8
m104	E S S W L D A F D I	0.7
m105	V G G I T G T A D A F D I	0.9
m106	D Q L A G Y Y Y D S S G Y H Y Y Y Y G M D V	1.6
m107	D H V H G P D A F D I	0.6
m108	V G G A F D I	0.5
m109	G W F R D W Y F D L	0.0
m110	E G L P E T D D A F D I	0.0
m111	E G A D Y	0.0
m112	D G A D Y	0.4
m113	Y K L Q S D A F D I	0.1
m114	A G P V G A T T G T F D Y	0.0
m115	G S Q S Y D H Y Y Y Y	0.4
m116	D S A G L G A	0.3
m117	R E S G P E F F Q H	0.0

[a] Screening of 380 individual phage clones was performed in a phage ELISA with sG as described in Materials and Methods. The sequences of the HC CDR3s (H3s) of phage-displayed Fabs that exhibited significant binding to sG in the phage ELISA are shown, as identified according to the IMGT database (http://imgt.cines.fr). Soluble Fabs were expressed, purified, and tested in the ELISA for binding to sG. The solution absorbance at 450 nm (A_{450}) is shown as a measure of the strength of binding.

are IgM specific. The light chains were from all Ig classes and showed greater variation compared to the germ line light chains (Table 2).

Inhibition of HeV Env-mediated fusion by the selected Fabs. To test the neutralizing activity of the antibodies, we first measured their ability to inhibit fusion mediated by HeV Env-expressing cells with cells that we had previously identified as fusion competent. Fusion was measured by two assays: a reporter gene assay and a syncytium formation assay. The seven Fabs that bound strongly to sG (Table 1) also exhibited measurable inhibitory activity in the reporter gene assay (Table 3) and were selected for further characterization. They also inhibited syncytium formation to various degrees, in general correlation with the inhibitory activity measured by the reporter gene assay (data not shown) (see below). Interestingly, six of the seven Fabs also inhibited to various degrees NiV Env-mediated fusion (Table 3). One antibody, m101, was most active against HeV Env-mediated fusion, while another one, m102, exhibited the highest cross-inhibitory activity against both HeV- and NiV Env-mediated fusion.

Neutralization of HeV and NiV by Fabs. The inhibitory activity of these Fabs was further tested by using infectious HeV and NiV in a neutralization assay as described in Materials and Methods. When tested at concentrations above 80 μg/ml, Fab m101 showed neutralizing activity against HeV but not against NiV, and Fab m102 exhibited weaker neutralizing activity against HeV compared to m101; at 30 μg/ml m101 exhibited 80% neutralizing activity against HeV, while m102 exhibited 30% against both HeV and NiV. Interestingly, as in the cell fusion assay, m102 exhibited cross-neutralizing activity for both HeV and NiV. The other tested Fabs did not show measurable neutralizing activity when tested at concentrations up to 100 μg/ml (data not shown). These results suggested that two of the selected Fabs could neutralize infectious HeV and NiV.

TABLE 2. V-gene families and amino acids changed compared to the germ line[a]

Antibody	VH family	VL family	No. of VH changes	No. of VL changes
m101	VH1	Vk1	2	6
m102	VH1	Vk3	5	8
m103	VH3	Vk2	0	0
m104	VH1	Vk2	0	13
m105	VH3	Vk1	0	0
m106	VH1	Vk1	0	0
m107	VH1	Vλ1	1	3

[a] Shown are the gene families for the VH genes, which are IgM specific, and for the VL genes, which are from all Ig classes, and their variations compared to germ line sequences.

TABLE 3. Inhibition of HeV Env-mediated cell fusion by the selected Fabs[a]

Fab	HeV	NiV
m101	+++	+
m102	++	++
m103	+	0
m104	+	+
m105	0	+
m106	+	++
m107	0	+
m108-17	0	0
X5	0	0

[a] Anti-HeV G Fabs were used for inhibition of fusion as described in Materials and Methods. A summary of four different experiments is shown, where each + is a measure of increased inhibitory activity and 0 means no measurable fusion activity compared to the background. Fab X5 is a control antibody specific for the human immunodeficiency virus type 1 gp120 (29).

Potent inhibitory activity of IgG1 m101 against HeV Env-mediated fusion and live virus. In most cases, but not always, whole antibodies are better neutralizers than Fabs. Thus, the most potent HeV-fusion-inhibiting Fab, m101, was converted to a whole antibody format (IgG1) and tested in a cell fusion assay. The IgG1 m101 inhibitory activity was much higher than the activity of the Fab m101 (Fig. 1 and 2). The conversion of Fab m101 to IgG1 dramatically decreased its 50% inhibitory concentration (IC_{50}). For HeLa-ATCC cells, which exhibit lower fusion rates, the IC_{50} decreased from 4.2 μg/ml to 0.5 μg/ml (Fig. 1A). For the highly fusogenic PCI-13 cells, the IC_{50} decreased from 38 μg/ml to 1.2 μg/ml (Fig. 1B). In another experiment the IgG1 m101 inhibited 95% of fusion at 3 μg/ml (data not shown). IgG1 m101 also potently inhibited syncytium formation in correlation with its inhibitory activity measured by the reporter gene assay. An example using the highly fusogenic PCI-13 cells is shown in Fig. 2. Here, IgG1 m101 completely inhibited formation of syncytia at 10 μg/ml, whereas at the same concentration, Fab m101 inhibited 50% of syncytium formation. This result approximately correlates with the data from the reporter-based fusion assay: notice that at 10 μg/ml the inhibition of fusion measured by this assay is 90% for the IgG1 m101 and 60% for the Fab m101 (Fig. 1B). However, this correlation is not absolute, because for PCI-13 cells the reporter-based fusion assay still detects some fusion, even at concentrations up to 50 μg/ml, where we have not observed formation of syncytia, although formation of doublets or triplets of fused cells may not be detected as syncytia.

IgG1 m101 was also exceptionally potent in neutralizing infectious HeV. Using a sensitive immunostaining plaque re-

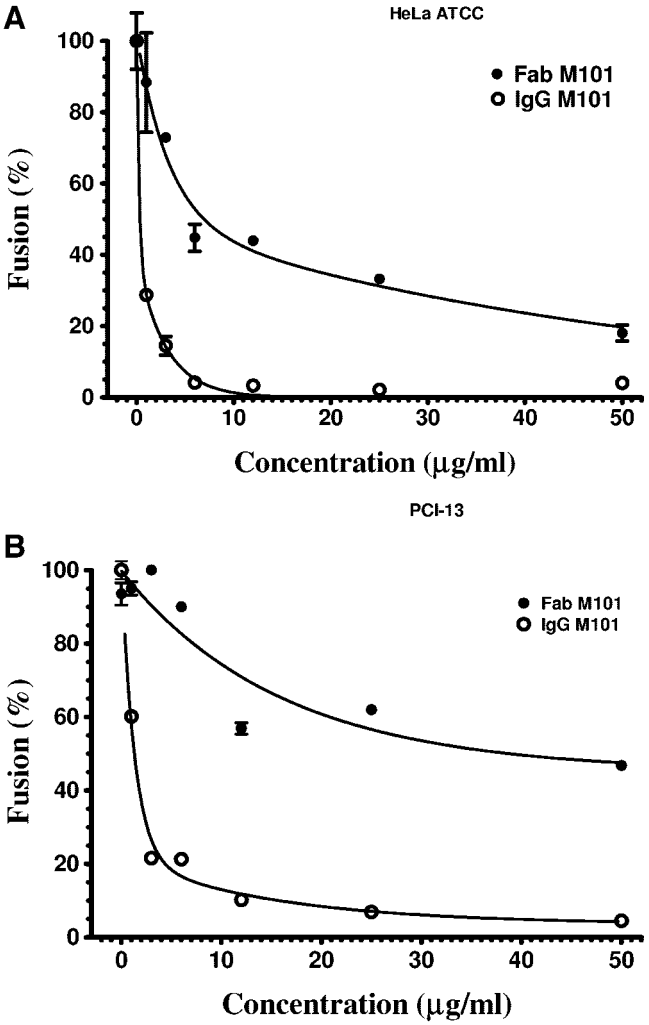

FIG. 1. There was significantly higher inhibitory activity of IgG1 m101 than Fab m101 in HeV Env-mediated cell fusion. HeLa-USU cells were infected with vaccinia virus recombinants encoding HeV F and G glycoproteins and with a vaccinia virus recombinant encoding T7 RNA polymerase (effector cells). Each designated target cell type was infected with the *E. coli* LacZ-encoding reporter vaccinia virus vCB21R. IgG1 m101 and Fab m101 were preincubated with effector cells and then mixed with target cells. The cell fusion assay was performed for 2.5 h at 37°C. Fusion was measured as described in Materials and Methods. Inhibition of HeV Env-mediated fusion by IgG1 m101 and Fab m101 in HeLa-ATCC cells (A) and in PCI-13 cells (B) is shown. Percentage of fusion is shown as a function of the antibody concentration. The curves represent the best fit of the experimental data from which IC_{50}s were calculated using Prism GraphPad software.

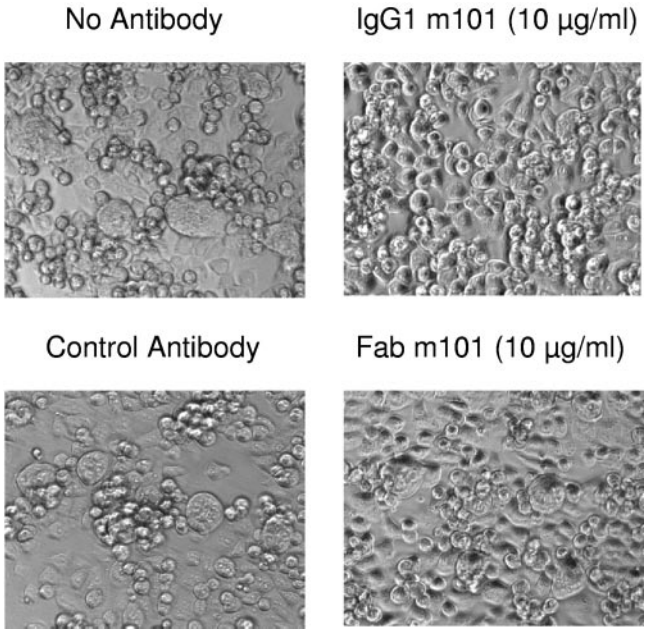

FIG. 2. Inhibition of HeV Env-mediated syncytium formation by m101. The effector cells, prepared as described in the Fig. 1 legend, were preincubated with IgG1 m101, Fab m101, or the control irrelevant antibody (X5, specific for human immunodeficiency virus [29]) for 20 min at room temperature, and then 2×10^5 cells in 200 μl were overlaid on 80% confluent monolayers of PCI-13 cells plated in a 48-well plate and incubated for 3 h at 37°C in a humidified 5% CO_2 atmosphere. Photographs were taken using a phase-contrast microscope with a 10× objective. Shown are illustrative portions of the original photographs electronically amplified for clarity. The top and bottom pictures of the left panel show formation of syncytia in the absence of antibody or in the presence of a control antibody; there were 17 or 20 giant fused cells (syncytia) counted per complete photograph view, respectively. The top and bottom pictures of the right panel show complete inhibition of syncytium formation by IgG1 m101 or reduction in the number of syncytia by Fab m101 at 10 μg/ml; there were 0 or 9 syncytia per complete view, respectively.

duction assay, complete (100%) neutralization was achieved at 12.5 μg/ml, more than 99% at 6 μg/ml, and 98% at 1.6 μg/ml (Table 4). These results demonstrated that IgG1 m101 is a very potent neutralizer of infectious HeV.

Mechanism of virus entry inhibition by antibodies: correlation with binding to native G. To begin to elucidate the mechanisms of the inhibitory activity of the selected antibodies, we measured their binding rate constants and affinities to sG in a Biacore assay. The antibodies bound with high (1 to 10^3 nM range) affinity to sG as measured by Biacore (Table 5). The on rate constants varied significantly, but there was no significant variation in the off rate constants, except the very low dissociation rate constant of m102. The best inhibitors of HeV G-mediated fusion and infection, m101 and m102, exhibited the highest affinities. In this context there was correlation

TABLE 4. Neutralization of infectious HeV by IgG1 m101[a]

Antibody concn (μg/ml)	No. of foci/well in each replicate	Avg no. of foci (% neutralization)
25	0, 0, 0, 0	0 (100)
12.5	0, 0, 0, 0	0 (100)
6.2	0, 0, 1, 0	0.25 (99)
3.1	1, 0, 1, 0	0.5 (98)
1.6	1, 1, 0, 0	0.5 (98)
0.8	5, 2, 2, 2	2.75 (91)
0	30, 37, 34, 30	33 (0)

[a] IgG1 m101 was incubated with infectious HeV, and the mixture was added to plated Vero cells. After the 30-minute incubation, antibody-virus mixtures were removed, cells were washed, and fresh EMEM-10 containing fresh antibody was added to the cells and incubated overnight. The average number of foci in the absence of antibody was 33. The percentage of neutralization shown below in parentheses was calculated by subtracting the number of foci in the wells with antibodies from the number of foci without antibodies, dividing the resulting number by the number of foci without antibodies, and multiplying by 100.

TABLE 5. Binding rate constants and affinities of selected Fabs[a]

Antibody	k_a (10^4) ($M^{-1} \cdot s^{-1}$)	k_d (10^{-3}) (s^{-1})	K_d (nM)
m101	13	3.5	28
m102	5.7	0.068	1.2
m103	*	*	1800
m104	0.3	1.6	600
m105	7.4	5.1	69
m106	6.2	3.3	54
m107	30	2.2	78

[a] Interaction between various Fabs and sG was analyzed at 25°C by surface plasmon resonance technology. Fabs at different concentrations were injected at flow rate of 30 μl/min, and the association and dissociation phase data were fitted simultaneously to a 1:1 Langumir global model by using the nonlinear data analysis program BIAevaluation 3.2. The individual association rate constant, k_a, dissociation rate constant, k_d, and equilibrium dissociation constant, K_d, were obtained from at least three separate experiments. The standard deviation was on average about 20%. *, only steady-state affinity was calculated due to fast kinetics.

between binding to sG and fusion inhibition by groups of antibodies divided into good (m101 and m102) and poor (the rest) neutralizers, although directly mathematically calculated correlation between the Biacore-measured affinity of each antibody to sG and fusion inhibitory activity was not found.

To find other possible correlations between binding and inhibition, we measured binding to native G, which was immunoprecipitated from lysates of cells infected with recombinant vaccinia viruses. The extent of immunoprecipitation, which is proportional to the antibody binding affinity to native full-length G glycoprotein, was highest for m101 binding to HeV G (Fig. 3 and data not shown). Two of these antibodies, m102 and m106, demonstrated significant cross-reactivity to both HeV and NiV G (Fig. 3). The levels of immunoprecipitation correlated with cell fusion (Table 3), suggesting that binding to native G is a better correlate of fusion inhibitory activity than binding to soluble G.

Outcompeting the receptor ephrin-B2 as a mechanism of virus entry inhibition by m101 and m102. To further define the mechanism of virus entry inhibition by the most potent neutralizer, m101, we measured its competition with the recently identified receptor for Hendra and Nipah viruses, ephrin-B2 (5, 31). m101 competed with ephrin-B2 for binding to sG; IgG m101 was a much better competitor than Fab m101 (Fig. 4), which correlates with their inhibitory activities and is likely due to the multivalent nature of their interaction. Similar results were obtained with m102 (data not shown) and by using Biacore (data not shown; see supplemental Fig. 2 in reference 5). These data suggest that m101 and m102 inhibit entry of Hendra virus and likely Nipah virus by preventing the access of these viruses to their receptor. They also suggest that the epitopes of m101 and m102 overlap with the receptor binding site on G. Interestingly, m106 competed with ephrin-B2 much more weakly than m101 and only at very high concentrations (Fig. 4).

Further characterization of epitopes of selected anti-G antibodies. To further characterize the epitopes of the newly identified antibodies, we measured the competition of m101, m102, m103, m106, and m107 with one another by ELISA (presently, there are no anti-HeV G antibodies with known epitopes). The m101, m102, and m103 antibodies competed with each other, suggesting that they bind to overlapping

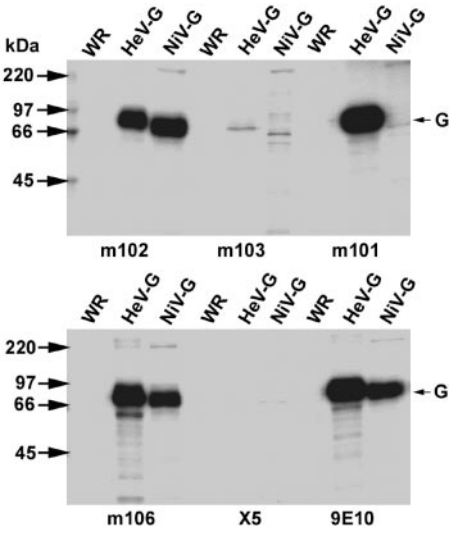

FIG. 3. Immunoprecipitation of HeV and NiV G glycoproteins by anti-G Fabs. HeLa cells were infected with WR, a control vaccinia virus, or recombinant vaccinia virus expressing myc-tagged HeV G or NiV G and, beginning at 6 h postinfection, labeled with [^{35}S]methionine-cysteine at 37°C overnight. Lysates were made in buffer containing Triton X-100 and incubated with various Fabs or mouse anti-myc 9E10 for at least 1 h at 4°C and then precipitated with protein G-Sepharose. Immunoprecipitated proteins were analyzed by 10% SDS-PAGE followed by autoradiography. WR denotes a control where the cells were infected with wild-type vaccinia virus, X5 is a control antibody specific for gp120 of human immunodeficiency virus, and 9E10 is an anti-c-Myc antibody serving as a positive control. The arrows next to G denote the positions of the bands corresponding to the monomeric G.

epitopes which are distinct than the epitopes of m106 and m107 (Table 6). Interestingly, m103 appears to synergize with m106, leading to increased binding of one in the presence of the other (data not shown). These results suggest that m101 to -3 may neutralize the virus by a different mechanism than m106

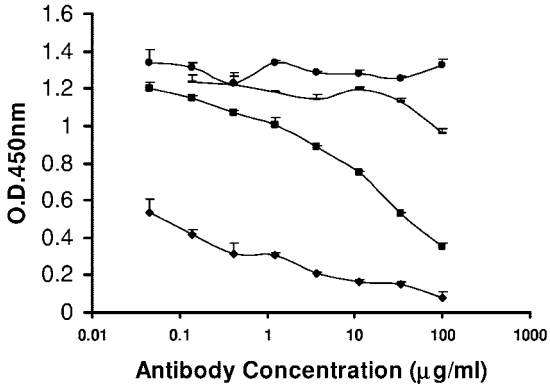

FIG. 4. Competition between anti-G antibodies and ephrin-B2 for binding to HeV G. Serially diluted Fab m101 (squares), IgG1 m101 (diamonds), and Fab m106 (horizontal bars) were mixed with HeV G and added to the virus receptor ephrin-B2 coated on the bottom of a 96-well plate, and the amount of bound G was measured as described in Materials and Methods. A Fab specific for the severe acute respiratory syndrome coronavirus S protein (circles) was used as a control.

TABLE 6. Competition of m101, m102, m103, m106, and m107 with one another[a]

Fab	Effect on binding to:				
	m101	m102	m103	m106	m107
m101	+	+	+	0	0
m102	+	+	+	0	0
m103	+	+	+	−	−/0
m106	0	0	−	+	+/0
m107	0	0	+	+/0	+

[a] Anti-HeV Fabs were coated in 96-well plates, and mixtures of c-Myc-tagged sG and competing Fab were added to each coated well. After washing, the bound sG was detected with horse radish peroxidase-conjugated anti-c-Myc antibody. The results are a summary of two independent experiments, where − denotes enhancement of binding, + denotes competition, and 0 indicates a lack of measurable effect on the Fab binding by the other Fab.

and m107, but further studies are needed to definitely elucidate the mechanism of their neutralizing activity.

In an initial attempt to localize the epitopes of m101 and m102, we measured their binding to a panel of 11 G alanine-scanning mutants, selected to represent different portions of the protein: G183A, L184A, P185A, (Q191 K192A), S195A, D289A, K324A, (I385 H386A), S447A, L517A, and N570A, where the two double mutants are in parentheses. Of these mutants two, P185A and Q191 K192A, decreased binding of m101 to G more than twofold; these mutants bound strongly to

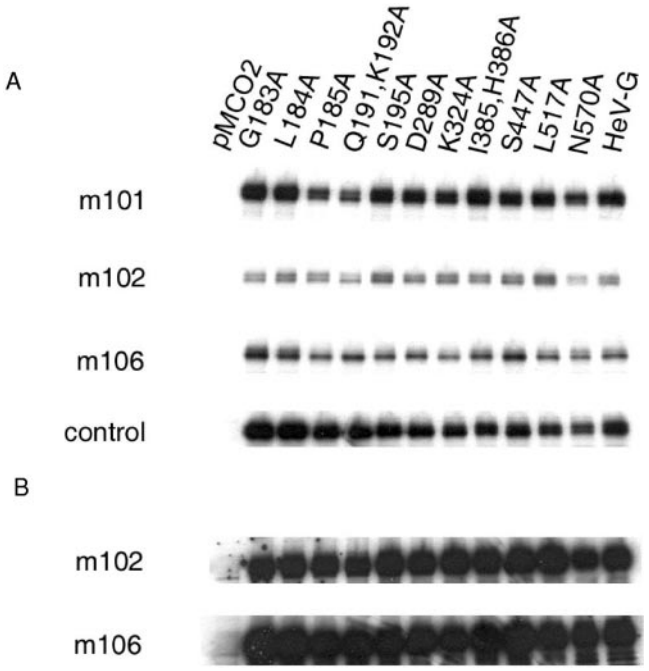

FIG. 5. Binding of m101 and m102 to alanine mutants of HeV G. HeLa cells transfected with wild-type HeV G, various alanine mutants of HeV G, or pMCO2 (empty vector) were infected with WR vaccinia virus to drive expression, radiolabeled with [^{35}S]methionine-cysteine overnight, lysed in buffer containing Triton X-100, and then subjected to immunoprecipitation by m101, m102, or rabbit polyclonal G antisera. Lysates were then precipitated with protein G-Sepharose and analyzed by 10% SDS-PAGE followed by autoradiography. (A) Gels after short (10-h) exposure; (B) m102 and m106 after a long (2-week) exposure.

TABLE 7. Binding of antibodies to alanine-scanning HeV-G mutants[a]

Mutant	Rel amt bound G		
	m101	m102	m106
G183A	0.76	**0.49**	1.06
L184A	0.72	0.52	0.88
P185A	**0.50**	0.60	0.72
Q191 K192A	**0.49**	0.56	0.92
S195A	0.84	0.70	0.79
D289A	0.90	0.82	0.90
K324A	0.90	0.99	0.77
I385 H386A	1.24	0.99	1.30
S447A	0.93	1.05	1.44
L517A	1.26	1.27	1.17
N570A	1.07	1.11	1.09
WT HeV	1.00	1.00	1.00

[a] The area under the peak for each mutant and the wild-type (WT) HeV G was scanned and normalized to the respective peaks with the polyclonal antibody. Then, all ratios were normalized to WT by dividing with the ratio for the WT. The values represent the relative amount of bound G mutants by the antibodies. Two independent experiments were performed for m101 and m102 with variations less than 30%. The ratios shown here correspond to data in Fig. 5A for m101 and m106 and Fig. 5B for m102. Mutants with more than a 50% decrease in binding are indicated in bold for the respective antibody.

anti-G rabbit polyclonal antibodies and to the receptor ephrin-B2 (Fig. 5, Table 7, and data not shown). The P185 residue is localized at the base of the globular head of the G protein, and the Q191 and K192 residues are located in the first portion of the globular head of G according to a model structure (36, 37), just following the stalk region, and either one or both could be a part of the antibody epitope that does not overlap with the receptor binding site on G. Another residue, G183, appears to decrease binding of m102 to G but not the binding of m101 and the receptor. This residue could be a part of the m102 epitope that does not overlap with the epitope of m101 and the receptor binding site on G. Three other G mutants, L184A, P185A, and Q191 K192A, exhibit close to but smaller than a 50% decrease in binding to m102 and are under further investigation for their role in the m102 interaction with G. None of the mutants tested appeared to affect significantly the G binding ability to m106. Further, more quantitative analysis with a larger panel of mutants is in progress to finely map the epitopes of these antibodies.

DISCUSSION

The major finding of this study is the identification of an antibody, m101, with exceptional potency against infectious HeV. Six other antibodies were also identified that are specific for HeV G, and two of them significantly cross-reacted with NiV G. To our knowledge, these antibodies are the first hMAbs identified against HeV and NiV. Interestingly, the only monoclonal antibody approved by the FDA for clinical use against a viral disease, Synagis (palivizumab; MEDI-493) (17, 33), is also specific for a paramyxovirus, respiratory syncytial virus (RSV); it is a humanized version of a mouse antibody and is used for prevention of RSV infections in neonates and immune-compromised individuals. Synagis inhibits virus entry and cell fusion in vitro very potently; it appears that its efficacy in vivo is correlated to its potency in vitro, and it was proposed that its fusion-inhibiting activity could be a major determinant

of its potency in vivo (25). Because RSV and henipaviruses enter cells by the same pathway, by fusion at the cell surface and not through endocytosis as most other enveloped viruses do, and are members of the same virus family, one might speculate that m101 could be equally if not more effective against HeV as palivizumab is against RSV.

Each of the newly identified Fabs was examined in HeV- and NiV-mediated cell fusion assays to evaluate their potential in blocking binding and/or the subsequent membrane fusion process. The Fab m101 demonstrated the most potent cell-fusion inhibitory activity, and m102 exhibited cross-reactive activity against both HeV and NiV. Another antibody, m106, also exhibited a certain degree of cross-reactivity. Notably, these three antibodies, which also bound to the G protein with highest strength, contain Y-rich long H3, unlike the others; whether this contributes to the mechanism of binding and how are currently under investigation. The mechanism by which m101 and m102 inhibit HeV fusion and infection is by blocking the interaction of G with ephrin-B2, which was recently identified as a functional receptor for HeV and NiV (5, 31). However, an additional possibility is that these antibodies bind to G and can also prevent its required interaction with the F glycoprotein to trigger the fusion process. There was a general correlation between their inhibitory activity and binding affinity of the Fabs to the G glycoprotein, especially to the native membrane-associated protein as measured by immunoprecipitation.

Conversion of Fab m101 to IgG1 led to potent neutralization of infectious HeV, where it neutralized more than 90% at a concentration of less than 1 μg/ml. One could speculate that this may be due to increased stability and avidity of the antibody or/and its ability to cross-link the oligomeric G glycoprotein on the surfaces of virus and infected cells. Nonetheless, the extreme potency of IgG1 m101 in infectious HeV neutralization assays suggests that it may be important to convert other Fabs to IgG1 for evaluation as potent neutralizing hMAbs.

There is considerable amino acid homology between the F and G Envs of HeV and NiV (22, 35). Previous studies have demonstrated that HeV and NiV antisera do cross-neutralize, with each serum being slightly less effective against the heterotypic virus (16, 34). Further, the HeV and NiV glycoproteins can functionally complement one another in mediating membrane fusion with wild-type efficiency (6, 10). Thus, we anticipated that if antibodies were identified using sG from HeV, some should display cross-reactive binding to shared epitopes between HeV and NiV. Indeed, two of the seven Fabs were capable of reacting equally well in immunoprecipitation of recombinant membrane-associated HeV and NiV G. In addition, m102 was capable of inhibiting HeV- and NiV-mediated fusion and may reflect a conserved epitope between these viruses that could be important not only for neutralization but also for the entry mechanism. Perhaps upon conversion to an IgG1, m102 may be capable of potently neutralizing both HeV and NiV.

Antibody binding competition assays revealed that the panel of Fabs developed here comprise two distinct groups, and Fabs within each group possess overlapping epitopes. Analysis of the anti-G Fabs by Western blotting revealed no reactivity to G, indicating that the epitopes recognized by these Fabs are likely conformation dependent (data not shown). The most potent neutralizers, m101 and m102, bound to most of the alanine mutants tested except for a few which appear to be located at the base of the globular head of G localized and in the first portion of the globular head of G according to a model of its structure (36, 37). Further studies are needed to precisely localize their epitopes.

Taken together, our results demonstrate new potential immuno-therapeutics against HeV and NiV. These human antibodies could be also used for diagnosis, as research reagents, and to aid in the development of vaccines.

ACKNOWLEDGMENTS

This study was supported by the NIH NCI CCR intramural program, contract no. NO1-CO-12400, and the NIH Biodefense Program (D.S.D.) and by the Middle Atlantic Regional Center of Excellence for Biodefense and Emerging Infectious Disease Research, NIH AI057168 and USUHS R073IL grants (C.C.B.).

The views expressed in the manuscript are solely those of the authors, and they do not represent official views or opinions of the Department of Defense or The Uniformed Services University of the Health Sciences.

REFERENCES

1. **Anonymous.** 1999. Update: outbreak of Nipah virus–Malaysia and Singapore, 1999. Morb. Mortal. Wkly. Rep. **48:**335–337.
2. **Anonymous.** 2004. Nipah virus outbreak(s) in Bangladesh, January-April, 2004. Wkly. Epidemiol. Rec. **79:**168–171.
3. **Anonymous.** 2004. Person-to-person transmission of Nipah virus during outbreak in Faridpur District. Health and Science Bulletin (ICDDR, B) **2:**5–9.
4. **Anonymous.** 2005. Emerging infections update: November 2004 to January 2005. Commun. Dis. Rep. Wkly., vol. 15.
5. **Bonaparte, M. I., A. S. Dimitrov, K. N. Bossart, G. Crameri, B. A. Mungall, K. A. Bishop, V. Choudhry, D. S. Dimitrov, L. F. Wang, B. T. Eaton, and C. C. Broder.** 2005. Ephrin-B2 ligand is a functional receptor for Hendra virus and Nipah virus. Proc. Natl. Acad. Sci. USA **102:**10652–10657.
6. **Bossart, K. N., and C. C. Broder.** 2004. Viral glycoprotein-mediated cell fusion assays using vaccinia virus vectors. Methods Mol. Biol **269:**309–332.
7. **Bossart, K. N., G. Crameri, A. S. Dimitrov, B. A. Mungall, Y. R. Feng, J. R. Patch, A. Choudhary, L. F. Wang, B. T. Eaton, and C. C. Broder.** 2005. Receptor binding, fusion inhibition, and induction of cross-reactive neutralizing antibodies by a soluble G glycoprotein of Hendra virus. J. Virol. **79:**6690–6702.
8. **Bossart, K. N., B. A. Mungall, G. Crameri, L. F. Wang, B. T. Eaton, and C. C. Broder.** 2005. Inhibition of Henipavirus fusion and infection by heptad-derived peptides of the Nipah virus fusion glycoprotein. Virol. J. **2:**57.
9. **Bossart, K. N., L. F. Wang, B. T. Eaton, and C. C. Broder.** 2001. Functional expression and membrane fusion tropism of the envelope glycoproteins of Hendra virus. Virology **290:**121–135.
10. **Bossart, K. N., L. F. Wang, M. N. Flora, K. B. Chua, S. K. Lam, B. T. Eaton, and C. C. Broder.** 2002. Membrane fusion tropism and heterotypic functional activities of the Nipah virus and Hendra virus envelope glycoproteins. J. Virol. **76:**11186–11198.
11. **Butler, D.** 2004. Fatal fruit bat virus sparks epidemics in southern Asia. Nature **429:**7.
12. **Chew, M. H., P. M. Arguin, D. K. Shay, K. T. Goh, P. E. Rollin, W. J. Shieh, S. R. Zaki, P. A. Rota, A. E. Ling, T. G. Ksiazek, S. K. Chew, and L. J. Anderson.** 2000. Risk factors for Nipah virus infection among abattoir workers in Singapore. J. Infect. Dis. **181:**1760–1763.
13. **Chua, K. B., W. J. Bellini, P. A. Rota, B. H. Harcourt, A. Tamin, S. K. Lam, T. G. Ksiazek, P. E. Rollin, S. R. Zaki, W. Shieh, C. S. Goldsmith, D. J. Gubler, J. T. Roehrig, B. Eaton, A. R. Gould, J. Olson, H. Field, P. Daniels, A. E. Ling, C. J. Peters, L. J. Anderson, and B. W. Mahy.** 2000. Nipah virus: a recently emergent deadly paramyxovirus. Science **288:**1432–1435.
14. **Chua, K. B., K. J. Goh, K. T. Wong, A. Kamarulzaman, P. S. Tan, T. G. Ksiazek, S. R. Zaki, G. Paul, S. K. Lam, and C. T. Tan.** 1999. Fatal encephalitis due to Nipah virus among pig-farmers in Malaysia. Lancet **354:**1257–1259.
15. **Chua, K. B., S. K. Lam, C. T. Tan, P. S. Hooi, K. J. Goh, N. K. Chew, K. S. Tan, A. Kamarulzaman, and K. T. Wong.** 2000. High mortality in Nipah encephalitis is associated with presence of virus in cerebrospinal fluid. Ann. Neurol. **48:**802–805.
16. **Crameri, G., L. F. Wang, C. Morrissy, J. White, and B. T. Eaton.** 2002. A rapid immune plaque assay for the detection of Hendra and Nipah viruses and anti-virus antibodies. J. Virol. Methods **99:**41–51.
17. **Dimitrov, D. S.** 2004. Virus entry: molecular mechanisms and biomedical applications. Nat. Rev. Microbiol. **2:**109–122.
18. **Eaton, B. T.** 2001. Introduction: current focus on Hendra and Nipah viruses. Microbes Infect. **3:**277–278.

19. **Enserink, M.** 2004. Emerging infectious diseases. Nipah virus (or a cousin) strikes again. Science **303:**1121.
20. **Field, H., P. Young, J. M. Yob, J. Mills, L. Hall, and J. Mackenzie.** 2001. The natural history of Hendra and Nipah viruses. Microbes Infect. **3:**307–314.
21. **Goh, K. J., C. T. Tan, N. K. Chew, P. S. Tan, A. Kamarulzaman, S. A. Sarji, K. T. Wong, B. J. Abdullah, K. B. Chua, and S. K. Lam.** 2000. Clinical features of Nipah virus encephalitis among pig farmers in Malaysia. N. Engl. J. Med. **342:**1229–1235.
22. **Harcourt, B. H., A. Tamin, T. G. Ksiazek, P. E. Rollin, L. J. Anderson, W. J. Bellini, and P. A. Rota.** 2000. Molecular characterization of Nipah virus, a newly emergent paramyxovirus. Virology **271:**334–349.
23. **Hooper, P., S. Zaki, P. Daniels, and D. Middleton.** 2001. Comparative pathology of the diseases caused by Hendra and Nipah viruses. Microbes Infect. **3:**315–322.
24. **Hsu, V. P., M. J. Hossain, U. D. Parashar, M. M. Ali, T. G. Ksiazek, I. Kuzmin, M. Niezgoda, C. Rupprecht, J. Bresee, and R. F. Breiman.** 2004. Nipah virus encephalitis reemergence, Bangladesh. Emerg. Infect. Dis. **10:** 2082–2087.
25. **Johnson, S., S. D. Griego, D. S. Pfarr, M. L. Doyle, R. Woods, D. Carlin, G. A. Prince, S. Koenig, J. F. Young, and S. B. Dillon.** 1999. A direct comparison of the activities of two humanized respiratory syncytial virus monoclonal antibodies: MEDI-493 and RSHZl9. J. Infect. Dis. **180:**35–40.
26. **Lamb, R. A., and D. Kolakofsky.** 2001. *Paramyxoviridae*: the viruses and their replication, p. 1305–1340. *In* D. M. Knipe and P. M. Howley (ed.), Fields virology. Lippincott Williams & Wilkins, Philadelphia, Pa.
27. **Lee, K. E., T. Umapathi, C. B. Tan, H. T. Tjia, T. S. Chua, H. M. Oh, K. M. Fock, A. Kurup, A. Das, A. K. Tan, and W. L. Lee.** 1999. The neurological manifestations of Nipah virus encephalitis, a novel paramyxovirus. Ann. Neurol. **46:**428–432.
28. **Lim, C. C., Y. Y. Sitoh, F. Hui, K. E. Lee, B. S. Ang, E. Lim, W. E. Lim, H. M. Oh, P. A. Tambyah, J. S. Wong, C. B. Tan, and T. S. Chee.** 2000. Nipah viral encephalitis or Japanese encephalitis? MR findings in a new zoonotic disease. Am. J. Neuroradiol. **21:**455–461.
29. **Moulard, M., S. K. Phogat, Y. Shu, A. F. Labrijn, X. D. Xiao, J. M. Binley, M. Y. Zhang, I. A. Sidorov, C. C. Broder, J. Robinson, P. W. H. I. Parren, D. R. Burton, and D. S. Dimitrov.** 2002. Broadly cross-reactive HIV-1-neutralizing human monoclonal Fab selected for binding to gp120-CD4-CCR5 complexes. Proc. Natl. Acad. Sci. USA **99:**6913–6918.
30. **Murray, K., P. Selleck, P. Hooper, A. Hyatt, A. Gould, L. Gleeson, H. Westbury, L. Hiley, L. Selvey, and B. Rodwell.** 1995. A morbillivirus that caused fatal disease in horses and humans. Science **268:**94–97.
31. **Negrete, O. A., E. L. Levroney, H. C. Aguilar, A. Bertolotti-Ciarlet, R. Nazarian, S. Tajyar, and B. Lee.** 2005. EphrinB2 is the entry receptor for Nipah virus, an emergent deadly paramyxovirus. Nature **436:**401–405.
32. **Nussbaum, O., C. C. Broder, and E. A. Berger.** 1994. Fusogenic mechanisms of enveloped-virus glycoproteins analyzed by a novel recombinant vaccinia virus-based assay quantitating cell fusion-dependent reporter gene activation. J. Virol. **68:**5411–5422.
33. **Pollack, P., and J. R. Groothuis.** 2002. Development and use of palivizumab (Synagis): a passive immunoprophylactic agent for RSV. J. Infect. Chemother. **8:**201–206.
34. **Tamin, A., B. H. Harcourt, T. G. Ksiazek, P. E. Rollin, W. J. Bellini, and P. A. Rota.** 2002. Functional properties of the fusion and attachment glycoproteins of Nipah virus. Virology **296:**190–200.
35. **Wang, L., B. H. Harcourt, M. Yu, A. Tamin, P. A. Rota, W. J. Bellini, and B. T. Eaton.** 2001. Molecular biology of Hendra and Nipah viruses. Microbes Infect. **3:**279–287.
36. **White, J. R., V. Boyd, G. S. Crameri, C. J. Duch, R. K. van Laar, L. F. Wang, and B. T. Eaton.** 2005. Location of, immunogenicity of and relationships between neutralization epitopes on the attachment protein (G) of Hendra virus. J. Gen. Virol. **86:**2839–2848.
37. **Yu, M., E. Hansson, J. P. Langedijk, B. T. Eaton, and L. F. Wang.** 1998. The attachment protein of Hendra virus has high structural similarity but limited primary sequence homology compared with viruses in the genus Paramyxovirus. Virology **251:**227–233.